JBC Papers in Press. Published on October 13, 2016 as Manuscript M116.741140
The latest version is at http://www.jbc.org/cgi/doi/10.1074/jbc.M116.741140

Hyper-activation of the insulin signaling pathway improves intracellular proteostasis by coordinately upregulating the proteostatic machinery in adipocytes

Annabel Y. Minard[1,2], Martin K. L. Wong[1,2,3], Rima Chaudhuri[2], Shi-Xiong Tan[1*], Sean J. Humphrey[2], Benjamin L. Parker[2], Jean Y. Yang[4], D. Ross Laybutt[1], Gregory J. Cooney[2], Adelle C.F. Coster[5], Jacqueline Stöckli[2] and David E. James[2,6]

[1]The Garvan Institute of Medical Research, Sydney, NSW 2010, Australia
[2]Charles Perkins Centre, School of Life Environmental Sciences, University of Sydney, Sydney, NSW 2006, Australia
[3]School of Physics, University of Sydney, Sydney, NSW 2006, Australia
[4]School of Mathematics and Statistics, University of Sydney, Sydney, NSW, 2006, Australia
[5]Department of Applied Mathematics, School of Mathematics and Statistics, University of New South Wales, Sydney, NSW 2052, Australia
[6]School of Medicine, University of Sydney, Sydney, NSW 2006, Australia
*Present address: School of Applied Science, Republic Polytechnic, Singapore 738964, Singapore

Running title: *Insulin-regulated proteostasis*

To whom correspondence should be addressed: David E. James, Charles Perkins Centre, School of Life Environmental Sciences, University of Sydney, Sydney, NSW 2006, Australia, Tel.: +61 2 8627 1621, E-mail: david.james@sydney.edu.au

Keywords: Insulin, insulin resistance, adipocyte, proteostasis, proteomics, pulse-chase SILAC

ABSTRACT

Hyperinsulinemia, which is associated with aging and metabolic disease, may lead to defective protein homeostasis (proteostasis) due to hyper-activation of insulin sensitive pathways such as protein synthesis. We investigated the effect of chronic hyperinsulinemia on proteostasis, by generating a time-resolved map of insulin-regulated protein turnover in adipocytes using metabolic pulse chase labelling and high-resolution mass spectrometry. Hyperinsulinemia increased the synthesis of nearly half of all detected proteins and did not affect protein degradation, despite suppressing autophagy. Unexpectedly, this marked elevation in protein synthesis was accompanied by enhanced protein stability and folding and not by markers of proteostasis stress such as protein carbonylation or aggregation. The improvement in proteostasis was attributed to a co-ordinate upregulation of proteins in the global proteostasis network, including ribosomal, proteasomal, chaperone and ER/mitochondrial UPR proteins. We conclude that defects associated with hyper-activation of the insulin signalling pathway are unlikely attributed to defective proteostasis because upregulation of protein synthesis by insulin is accompanied by upregulation of proteostatic machinery.

The insulin signalling pathway (ISP) is a master regulator of protein metabolism. Many of its effects, such as increased protein synthesis and reduced autophagy, are orchestrated via mTORC1 (1,2). The ISP is hyper-activated by chronic hyperinsulinemia, a common consequence of insulin resistance and aging (3). This in turn exacerbates insulin resistance, obesity (4-6) and aging (7-10). Chronic ISP activity may partially cause these detrimental effects by dysregulating protein homeostasis (proteostasis) (11,12). Supporting this view, genetic manipulations that lead to either endoplasmic reticulum (ER) stress, reduced proteasomal activity or reduced autophagy are associated with insulin resistance in mice (13-15). Moreover the mTORC1 inhibitor

rapamycin extends lifespan in a range of animals, and in *Drosophila* these effects are at least in part due to reduced protein synthesis and enhanced autophagy (16).

Proteins are made via a carefully orchestrated process that minimises misfolding. This involves chaperones that ensure efficient folding of newly synthesised proteins, the ubiquitin-proteasome system that degrades misfolded proteins, and autophagy for removal of protein aggregates (17,18). It has been proposed that chronic insulin signalling impairs protein folding and promotes aggregation, since it simultaneously activates protein synthesis, suppresses autophagy and inhibits the activity of FOXO, a transcription factor that regulates chaperone gene expression (11,12,19-21).

The effect of loss of function of daf-2/ISP activity on global proteostasis was recently studied in *C. elegans* (22), but few studies have examined the effects of hyper-activation of the ISP on proteostasis and none at a systems-wide level. Furthermore, the full complement of proteins that are synthesised and/or degraded in response to insulin have not been characterised. Here we investigated the global effects of hyperactive insulin signalling on protein synthesis and degradation using pulse-chase labelling with stable isotopes (SILAC) (23-28) and high-resolution mass spectrometry (MS)-based proteomics.

Our studies focus on post-mitotic 3T3-L1 adipocytes because exposure of these cells to chronic hyperinsulinemia results in insulin resistance (29) and defects in insulin action in adipocytes contribute to whole body insulin resistance (30). Moreover, while primary mouse/rat adipocytes lose their insulin sensitivity upon long term culturing (31), 3T3-L1 adipocytes are highly insulin responsive for long periods (32).

Unexpectedly, while insulin potently stimulated protein synthesis and suppressed autophagy, there was no evidence of protein aggregation or carbonylation. Rather, insulin induced the synthesis of cytosolic chaperones, ER UPR and mitochondrial UPR proteins, and this was associated with improved rather than impaired protein folding. We therefore suggest that hyper-activation of the ISP does not contribute to impaired proteostasis, as insulin coordinated protein biosynthesis with the upregulation of the proteostasis network.

RESULTS

Mapping large-scale protein synthesis and degradation

To assess the effect of chronic insulin signalling on global proteostasis, we exposed 3T3-L1 adipocytes to insulin over 4 d, and analysed protein turnover by pulse-chase metabolic labelling and mass spectrometry (Fig. 1*A*). Insulin caused sustained stimulation of protein biosynthetic pathways, as indicated by a marked increase in total cellular protein content and S6 phosphorylation (Fig. 1*B* & 1*C*). To measure global protein turnover, we metabolically labelled 3T3-L1 fibroblasts with ‘heavy’ isotopes of arginine and lysine (Arg 10/Lys 8, ‘heavy’, H) until complete incorporation had occurred, then differentiated the fibroblasts into adipocytes. ‘Heavy’-labelled cells were then switched into culture media containing ‘medium’ isotopes of Arg and Lys (Arg 6/Lys 4, ‘medium’, M) and harvested over a time-series. Consequently a decay in ‘heavy’ labelled proteins is indicative of protein degradation and an increase in ‘medium’ proteins reflects protein synthesis (Fig. 1*A*) (24).

The cell lysates were mixed with a reference sample of ‘light’-labelled adipocytes (‘light’, L) for proteomic analysis. The experimental and reference samples were mixed such that DNA, rather than protein content was constant since altered protein synthesis might affect normalisation by protein mass. The samples contained an equal number of cells, as histone abundance, which is proportional to DNA mass, was highly consistent between samples (Fig. 1*D*).

We identified a total of 6,550 proteins, of which 2,560 newly synthesised ‘medium’ proteins and 2,321 degraded ‘heavy’ proteins were quantified across at least 50% of the time-series (supplemental Table S1). ‘Medium’- and ‘heavy’-labelled proteins increased and decreased, respectively, over the time course, and intersected at ~72 h, suggesting half the pool of proteins turn over after 3 d (Fig. 1*E*).

Insulin treatment commenced 1 d prior to switching to ‘medium’ isotopes (the start of the chase). Insulin-treated adipocytes demonstrated a similar decrease in ‘heavy’-labelled proteins as compared to untreated cells, but a greater increase in ‘medium’-labelled proteins (Fig. 1*E*). These changes correspond to increased protein synthesis

with no change in protein degradation rates in response to insulin treatment.

Insulin enhances the synthesis and stability of newly-made proteins

To identify the primary insulin responsive proteins we derived synthesis rates by fitting the increase in 'medium' proteins to a variation of a kinetic model described previously (27,33). In this model, proteins are synthesised linearly and, once made, are subject to degradation (Fig. 2*A* & 2*B*). An example of the model fit for two proteins is shown in Fig. 2*B*. The initial increase in 'medium'-labelled squalene epoxidase was due to proteins synthesis (m_{syn}), and this eventually reached a plateau (steady-state) due to degradation of the newly synthesised protein (m_{deg}). In contrast, GLUT4 was synthesised more slowly, and did not exhibit a plateau and so the degradation component was not apparent (Fig. 2*B*). We modelled the degradation rate of 'medium'- and 'heavy'-labelled proteins separately, since the degradation of newly synthesised proteins (m_{deg}) may differ from pre-existing proteins (h_{deg}).

Of the initial 2,560 quantified 'medium' proteins, 1,445 fit the model with adj. $R^2 > 0.8$, and 752 fit with a more stringent adj. $R^2 > 0.9$ (Fig. 2*A*, supplemental Table S1). Manual inspection revealed that a cut-off of adj. $R^2 > 0.8$ was sufficient to eliminate proteins with irregular profiles over the time course. Proteins may have exhibited irregular time profiles because of inaccurate quantification due to low abundance or slow protein synthesis; or cycling of protein abundance such as occurs under circadian control (34). While proteins with irregular profiles may be of interest, here we focussed on proteins which fit our basic model of turnover. We classified proteins as insulin-regulated if the control and insulin treated samples fit separate models better than one model with both data combined (adj. $p < 0.0005$). Using this criteria, several proteins with synthesis rates known to be regulated by insulin were identified, including GLUT4 and GAPDH (35-37). In total, insulin regulated the levels of around 46% of the proteins modelled (663 out of 1,445 proteins).

Some studies of mTORC1-mediated protein synthesis have suggested that chronic activation of mTORC1 reduces protein synthesis, as either inhibitory proteostatic pathways are activated or there is increased degradation of newly made proteins due to increased misfolding (38-40). In contrast to this view, in insulin-stimulated 3T3-L1 adipocytes we observed that all but one of the 663 insulin-regulated proteins increased in abundance (median increase 49% after 48 h) (Fig. 2*C*). To determine whether this was due to increased synthesis (m_{syn}) and/or decreased degradation of newly made proteins (m_{deg}), we compared the probable parameter values for m_{syn} and m_{deg} and found that protein synthesis rates were specifically increased for 468 and decreased for 22 proteins, while degradation rates were decreased for 197 and increased only for 20 proteins (Fig. 2*D*). These data suggest that chronic insulin treatment enhances both the synthesis and stability of newly made proteins.

Insulin minimally affects protein degradation despite inhibiting autophagy

We next examined the degradation of the pre-made 'heavy' proteins for evidence of insulin-regulated protein degradation or proteome destabilisation (Fig. 3*A*). To achieve this, 'heavy' proteins were fitted to an exponential decay model. Interestingly, 27% of proteins approached a plateau greater than one quarter of their starting abundance after 96 h, and thus did not completely degrade. To allow the model to approach a non zero plateau we included the h_{syn} parameter, so that the plateau is given by h_{syn}/h_{deg}. The incomplete protein degradation may reflect discrete pools of proteins with different turnovers. This is not surprising since the majority of proteins exists in both protein complexes and in isolation (41). Alternatively, 'heavy' amino acids liberated by proteolysis may be reincorporated into protein. However, this seems unlikely since h_{syn} varied among proteins. By allowing incomplete degradation in our model, we estimated the half-life of the insulin receptor to be 11.7 h (S.D. 8.76-15.7), which is similar to previously observed values (42).

In contrast to earlier pulse-chase SILAC studies, we found many proteins were long-lived, with 38% of proteins (891 proteins) exhibiting no detectable degradation over a 96 h period (Fig. 3*B*, supplemental Table S2). Insulin had no detectable effect on the degradation of long-lived proteins. These included nuclear pore proteins and histones,

consistent with a recent report *in vivo* (43), as well as mitochondrial electron transport chain proteins.

Among the 'heavy'-labelled proteins, 544 proteins fit our model of protein degradation with adj. $R^2 > 0.8$ (Fig. 3*A*, 3*C*, supplemental Table S1). For these proteins the median half-life was 47 h (Fig. 3*D*). There was more variability in protein degradation compared to synthesis. Since both processes were measured using the same samples, it is likely that protein degradation occurs with greater biological variability in 3T3-L1 adipocytes. In comparison, earlier pulse-chase SILAC studies in dividing cells reported less variable protein degradation. This may be because cell division is associated with activation of ubiquitin ligases (44), and higher rates of protein turnover (23-28).

In contrast to the effects of insulin on protein synthesis, insulin modulated the degradation of only 34 proteins using adj. $p < 0.01$, and 9 using a more stringent cut off of adj. $p < 0.005$. Consistent with this, insulin did not significantly modulate proteasomal activity in adipocytes (Fig. 3*E*). However, insulin suppressed autophagy, as indicated by the significant reduction in autophagic flux (Fig. 3*F*). Autophagic flux was measured by the difference in LC3-II, a marker of autophagosomes, with and without an inhibitor of autophagic degradation, chloroquine. Hence, these data indicate that insulin does not regulate global protein degradation, and by extension insulin-mediated inhibition of autophagy does not have a major impact on the adipocyte proteome.

Insulin coordinates protein synthesis with the proteostasis network

Insulin increased the synthesis of proteins involved in glucose metabolism, including glycolysis, tricarboxylic acid cycle and the pentose phosphate pathway (Fig. 4*A*, supplemental Table S3). Insulin also increased the synthesis of proteins that support protein synthesis and the clearance of misfolded proteins. These included ribosomal, tRNA biosynthetic, proteasomal proteins, ER and Golgi proteins that regulate homeostasis of the secretory/biosynthetic tract, as well as proteins involved in heat shock, mitochondrial and ER unfolded protein response (UPR). The expression of these proteins was proportional to the overall increase in cellular protein synthesis. As protein synthesis was not impaired, but rather significantly enriched in the cytosol, ER and Golgi compartments, it seems likely that elevated expression of these proteins is part of a coordinated response to support protein synthesis.

The up-regulation of ER UPR proteins was not associated with PERK activation as phosphorylation of neither PERK nor its substrate EIF2α was increased, but rather IRE1 phosphorylation was increased (Fig. 4*B*). These data are interesting as PERK reportedly promotes apoptosis, while IRE1 is cytoprotective (45). We examined whether hyperinsulinemic rats also exhibited ER UPR activation in adipose tissue. Previously rats were cannulated and infused with glucose (40 mg/kg/min) for 1 d or 4 d, resulting in a state of chronic *in vivo* hyperinsulinemia (Fig. 4*C*) (46) and chronic mTORC1 signalling in adipose, as indicated by elevated S6 phosphorylation after 1d and 4d glucose infusion, although changes after 4d were insignificant due to high variation (Fig. 4*D*). Akt phosphorylation was unchanged probably because of negative feedback in response to chronic insulin signalling. In adipose tissue from 1 d or 4 d hyperglycemic hyperinsulinemic rats, phosphorylation of IRE1, but not EIF2α, was increased compared to saline-infused rats (Fig. 4*D*). IRE1 phosphorylation was not induced by a proteostasis stress as IRE1 phosphorylation was increased after 30 sec insulin stimulation in 3T3-L1 adipocytes (Fig. 4*E*), well before mTORC1 activation (47). In addition, IRE1 phosphorylation was not inhibited by cycloheximide, an inhibitor of protein synthesis or by the mTORC1 inhibitor rapamycin (Fig. 4*F*). Rather, IRE1 phosphorylation was induced by PI3K/AKT activity, since it was blocked by inhibitors of Akt (MK2206) and PI3K/mTOR (LY294002) but not by inhibitors of MAPK (U0126) (Fig. 4*G*).

Therefore, we speculate that the activation of UPR proteins by insulin is not indicative of protein misfolding or cellular stress, but likely represents part of a coordinate proteostatic response, which may be regulated by IRE1 in preparation for a burst of insulin-regulated protein synthesis.

Protein synthesis via insulin and mTORC1 does not increase protein misfolding

To test the hypothesis that a burst of protein synthesis in response to insulin is accompanied by a coordinate proteostatic response, we next examined protein folding. Misfolded proteins often assemble into large insoluble aggregates that can be readily detected using a detergent solubility assay. As expected we observed a 4-fold increase in detergent insoluble proteins in cells treated with the proteasomal inhibitor MG132. However, we found no detectable increase in detergent insoluble proteins in cells treated with insulin for 4d (Fig. 5*A*). Similarly, there was no change in detergent insoluble protein in adipose tissue from glucose infused hyperinsulinemic rats (Fig. 5*B*). Next we examined protein carbonylation, a measure of cellular oxidative damage (Fig. 5*C*). Hydrogen peroxide caused a 2-fold increase in protein carbonylation in 3T3-L1 adipocytes, whereas no detectable increase was observed with insulin. Rather, insulin induced a small but significant reduction in protein oxidation, indicating an adaptive response against not only protein folding stress but also oxidative stress. Evidence for an adaptive anti-oxidant response was also found in our proteomic data: insulin up-regulated the antioxidants peroxiredoxin 4, carbonyl reductase 1 and 3 and a transcription factor enrichment analysis predicted activation of NRF2, which is involved in oxidative stress tolerance (supplemental Table S4). There was also no effect of *in vivo* hyperinsulinemia on protein carbonylation levels in rat adipose tissue (Fig. 5*D*). Collectively, these data indicate that chronic activation of insulin signalling is not accompanied by compromised protein synthesis or degradation, or a demonstrable change in markers of protein misfolding.

Since previous studies suggested that accelerated protein synthesis via mTORC1 causes protein misfolding, we reasoned that while the endogenous proteome was not detectably misfolded, insulin treatment might reduce folding capacity under stress. To test this hypothesis, we assayed folding in insulin treated adipocytes using firefly luciferase (Fluc). Luciferase is commonly used for measuring protein folding capacity as it folds rapidly upon translation and does not require post-translational modifications for its activity (48). The folding efficiency of wild type (WT) Fluc was not reduced by insulin treatment but instead demonstrated a trend toward increased synthesis (Fig. 5*F*). To further challenge the folding environment we expressed a destabilised luciferase construct (DM Fluc), which contains two point mutations that impair the ability of the protein to fold (49). DM Fluc had 5% of the activity of WT Fluc in control cells (Fig. 5*E*). Yet insulin treatment improved folding of DM Fluc by 50% (Fig. 5*G*). This increase was mTORC1-dependent since rapamycin abrogated the increase in DM Fluc folding (Fig. 5*H*). These data contrast with a report by Conn et al (38), where either chronic mTORC1 activation in TSC2-/- mouse embryonic fibroblasts or Rheb overexpression in HEK293 cells inhibited WT Fluc folding. To test whether our results were cell-type dependent, or if insulin differs in its response compared to selective and chronic mTORC1 activation, we expressed WT Fluc in HEK293 cells and measured folding in response to chronic insulin or Rheb overexpression. Both insulin and Rheb overexpression caused activation of mTORC1 but in neither case was folding significantly inhibited (Fig. 5*I-K*). Rather, Rheb overexpression led to an increase in WT Fluc activity, which was rapamycin insensitive. Based on our data, we suggest that increased translation associated with either chronic insulin or mTORC1 activation does not cause a reduction in proteins synthesised due to elevated misfolding, as has been previously proposed. Rather, both insulin and mTORC1 activity concurrently increase protein synthesis with the ability to fold proteins.

DISCUSSION

The ISP is a major regulator of protein metabolism, yet how hyper-activation of ISP, which occurs with aging and metabolic diseases, affects global proteostasis is unclear. To assess the effects of insulin on the composition, stability and folding of the proteome, we undertook a global analysis of protein synthesis and degradation, followed by assays to assess protein quality in 3T3-L1 adipocytes exposed chronically to insulin. Surprisingly, we found that insulin does not affect protein degradation, despite suppressing autophagy. Additionally, insulin increased synthesis of 46% of the proteome, without evidence of protein damage. Among the

upregulated proteins were many belonging to the proteostasis machinery including metabolic enzymes, protein chaperones, protein synthesis machinery and ER/Golgi proteins. Hence, this demonstrates that in response to chronic elevation of protein synthesis, cells possess adaptive mechanisms to cope with the additional protein folding burden by coordinately upregulating the proteostatic machinery.

The concept that the insulin signalling pathway is detrimental to health due to impaired protein misfolding stems largely from loss of function studies (22,50-53). Most notably, rapamycin is thought to extend lifespan in part by reducing protein synthesis and thus improving proteostasis (16). Based on these studies it has been inferred that increased insulin signalling would compromise cellular proteostasis. In the present study we tested the consequences of chronic hyper-activation of the insulin signaling pathway under well controlled experimental conditions using both adipocytes grown in culture and adipose tissue from hyperglycemic hyperinsulinemic rats and in neither case could we find evidence that hyper-activation of this pathway compromises cellular proteostasis. We assessed proteostasis by measuring insoluble proteins (Fig. 5*A*-*B*), protein carbonylation (Fig. 5*C*-*D*), synthesis of a destabilised luciferase construct (Fig. 5*G*) and stability of existing or newly made proteins in the MS-based map of proteome turnover (Fig. 2*D*, 3*A*). It has been shown that hyper-activation of the ISP reduces toxicity of misfolding-prone neurodegenerative proteins that have been expressed in various cell types, and so these studies are in general agreement with our findings that the ISP in fact promotes proteostasis (54-57). In contrast, it has been shown that constitutive hyper-activation of mTORC1 via either TSC2 deletion or overexpression of Rheb in HEK293 cells resulted in impaired protein folding although we have been unable to replicate the latter observation in the current study. The basis for why these findings contrast with the present findings remains unclear. However, aspects of proteostasis do appear to be inconsistent across studies using the chronic mTORC1 activation cell models (38-40,58). One possibility is that long-term overexpression of these hyper-activating mutants in cells over many generations results in ill-defined adaptive changes and it could be these changes that drive the proteostasis defect. Regardless, in our study, increased protein synthesis via either insulin or mTORC1 activation does not impair cellular proteostasis.

One of the reasons insulin was thought to cause protein misfolding is because it suppresses autophagy. Genetically inhibiting autophagy reduces protein degradation, thereby increasing protein aggregation (59,60). Here however, insulin had a relatively modest effect on overall protein degradation in adipocytes, indicating that insulin-dependent reduction in autophagy does not affect protein degradation.

We propose that cells accommodate the increased synthetic demand imposed by insulin by increasing synthesis of proteins involved in proteostasis, including chaperones and vesicle transport proteins. Initially, we expected that cytosolic chaperones would be down-regulated by chronic insulin as many of these are regulated by FOXO, a transcription factor that is suppressed by insulin. The insulin-dependent synthesis of chaperone proteins may instead be regulated via a pathway such as HSF1 or HIF1α. HSF1 was reported to be activated by mTORC1 following heat stress (61). Furthermore, HSF1 is induced during protein translation in various cancer cell lines (62). While it is possible that HSF1 may mediate the induction of the proteostasis network here, HSF1 was not significantly enriched in our transcription factor enrichment analysis (supplemental Table S4). Future studies examining this will be of considerable interest.

Insulin also up-regulated components of the mitochondrial and ER unfolded protein response. Previously activation of the ER UPR in adipose tissue in obese hyperinsulinemic subjects as well as in healthy subjects rendered acutely hyperinsulinemic was assumed to indicate compromised ER protein synthesis and stress and as a result proposed to cause insulin resistance (13,63-65). This is largely because the ER UPR was initially characterised as a response to agents such as tunicamycin and thapsigargin, which have a profound inhibitory effect on ER protein synthesis and cause insulin resistance (66). Our proteomic data reveal that insulin does not compromise ER protein synthesis. Rather, we propose that the induction of the ER UPR by insulin is part of a protective response and may be pre-emptively induced by Akt-mediated IRE1

phosphorylation in anticipation of a burst of protein synthesis. These observations are supported by other studies, which demonstrated that IGF-1 stimulates IRE1 phosphorylation to protect against ER stress and that the PI3K subunit p85α stimulates XBP1 splicing downstream of IRE1 phosphorylation, leading to resistance to ER stress (67,68). As such, activation of the ER UPR should not be used alone to indicate ER stress. Our data indicate that since hyperinsulinemia does not induce ER stress, ER stress is not likely to cause hyperinsulinemia induced insulin resistance. Additionally, ER stress during obesity is likely caused by factors aside from hyperinsulinemia.

In addition to examining the effects of insulin on proteostasis, we also explored the stability of the endogenous proteome of adipocytes. Proteins that were degraded in adipocytes had an average half-life of 47 h, which is similar to HeLa and NIH3T3 cells which are reported to have half-lives of 20 and 46 h, respectively (33,69). However, compared with these mitotic cells, we find that many proteins in adipocytes are highly stable: 24% of quantified proteins did not turnover during the 96 h period of investigation, and other proteins comprised a pool of protein that was resistant to degradation. This may suggest that proteins in post-mitotic cells, such as adipocytes, are particularly stable. This slow turnover of proteins may explain why knock down of proteins is difficult using siRNA in adipocytes; cells are typically exposed to siRNA for 2-3 days. We suggest that our global protein turnover data will be an invaluable guide for such experiments. The long-lived proteins are also of interest in the study of proteostasis as specialised repair mechanisms for the maintenance of long-lived proteins have not yet been identified.

The current study suggests that cellular proteostasis is a highly regulated process that can accommodate dynamic changes in protein turnover. Hyperinsulinemia increases protein biosynthesis, which has the potential to burden the proteostasis machinery. Here we show that insulin coordinately up-regulates the proteostasis network concomitant with protein synthesis. Therefore, the metabolic and health consequences of hyperinsulinemia are unlikely to be mediated by compromised proteostasis. Rather it seems likely that proteostasis defects are triggered by alternative mechanisms. In view of these data it seems unlikely that reduced protein synthesis accounts for the lifespan extending effects of loss of function mutations in the insulin signalling pathway or drugs such as rapamycin that dampen signalling downstream of the insulin receptor.

EXPERIMENTAL PROCEDURES

Cell culture

3T3-L1 adipocytes were cultured as described previously (47). For chronic insulin treatments, adipocytes were incubated with 10 nM insulin for 1-5 d with medium replenished every 12 h. For acute insulin treatments, 3T3-L1 adipocytes were serum starved in DMEM supplemented with 0.2% BSA for 2 h before incubation with 10 nM insulin. Inhibitors were added 30 min prior to insulin-stimulation, at the following concentrations: 10 µM cycloheximide (Sigma-Aldrich), 500 nM rapamycin (LC-Laboratories), 10 µM MK2206 (Sellekchem), 50 µM LY294002 (Tocris Bioscience), 10µM U0126 (Cell Signalling Technology). H_2O_2 (BDH) was used at 10 mM.

Pulse-Chase using stable isotopically labelled amino acids (SILAC)

SILAC DMEM (deficient in Lysine, Arginine and Leucine, Thermo Fisher) was supplemented with 10% dialysed FCS (Hyclone Laboratories), GlutaMAX (Life Technologies) and Leucine. Different isotopes of Arginine and Lysine were added to the DMEM to result in either 'light' (*L*) DMEM (Arg, Lys; Sigma), 'medium' (*M*) DMEM (Arg +6, Lys +4; Silantes) or 'heavy' (*H*) DMEM (Arg +10, Lys +8; Silantes). 3T3-L1 fibroblasts were passaged for six doublings in 'light' or 'heavy' SILAC DMEM and differentiated into adipocytes. On day 8 of differentiation, to commence the pulse-chase, 'heavy'-labelled adipocytes were washed 3 times in warm PBS and switched to 'medium' SILAC DMEM. Subsequently, 'medium' DMEM was replenished every 12 h. Cells were harvested at the following times after switching to 'medium' SILAC DMEM: 0, 6, 12, 24 and 48 h in the first experiment, and 0, 6, 12, 24, 48, 72 and 96 h in the second experiment. Insulin treated cells were exposed to 10 nM insulin for 24 h prior to start of the chase and thereafter.

Harvested cells were washed 3 times with ice cold PBS and solubilised by sonication in HES buffer (20 mM HEPES, pH 7.4, 1 mM EDTA, 250

mM sucrose) and protease inhibitors (Roche). DNA content was measured by Sybr Green I Nucleic Acid stain (S-7585, Thermo Fisher) assay using salmon sperm DNA (D1626, Sigma) as standards. Samples were mixed with 'light'-labelled adipocytes (reference cells) at a ratio of 1:1 based on DNA content and SDS was added (final conc. 2% w/v). Following mixing, proteins were processed by filter-aided sample preparation, trypsin digested (Promega), and peptides fractionated by Strong Anion Exchange (SAX) as described previously (70).

Mass Spectrometry (MS)

LC-MS/MS analysis was carried out on an LTQ-Orbitrap Velos Pro (Thermo Fisher Scientific) as described previously (47). Raw mass spectrometry data were processed using MaxQuant (71) version 1.3.0.5 using default settings except for: Oxidised Methionine (M), Acetylation (Protein N-term) which were selected as variable modifications, and Carbamidomethyl (C) as well as triple SILAC labels were set as fixed modifications. A maximum of two missed cleavages was permitted, 10 peaks per 100 Da, MS/MS tolerance of 20 ppm, and a minimum peptide length of 7. Database searching was performed using the Andromeda search engine integrated into the MaxQuant environment (72), against the mouse UniProt database (July 2013). Protein, peptide and site FDR thresholds in MaxQuant were each set to a maximum of 1%.

Modelling of synthesis and degradation rates

The MS data set contained 2 time courses of *H/L* and *M/L* proteins both under control and insulin conditions. Each time course was normalised to starting amounts of *H/L* in control, log2 transformed and normalised using LOESS curve fit. Proteins with ≥ 50% missing values in a time course were removed. The resulting data was fitted to a kinetic model of protein synthesis and degradation described by the ordinary differential equations:

$$[\dot{M}] = m_{syn} - [M]m_{deg} \quad (1)$$

$$[\dot{H}] = h_{syn} - [H]h_{deg} \quad (2)$$

Where $[\dot{M}]$ is the rate of change of the concentration of *M*-labelled proteins of interest and m_{syn} and m_{deg} are their synthesis and degradation rate constants, respectively. Similarly $[\dot{H}]$ is the rate of change of the concentration of *H*-labelled proteins and h_{syn} and h_{deg} are their corresponding synthesis and degradation rate constants. The differential equations were solved with the initial conditions $[M](0) = 0$ and $[H](0) = 1$ to obtain the following models:

$$[M] = \frac{m_{syn}}{m_{deg}}\left[1 - \exp(-m_{deg}t)\right] \quad (3)$$

$$[H] = \frac{h_{syn}}{h_{deg}} + \left(1 - \frac{h_{syn}}{h_{deg}}\right)\exp\left(-h_{deg}t\right) \quad (4)$$

The data was fitted to the models and optimal parameters obtained by minimising the weighted least squares residual (ε) using the Nelder-Mead simplex method in MATLAB version R2015a (The MathWorks Inc.). The half-life of proteins was determined as $\ln 2 \,/ m_{deg}$.

Statistical identification of insulin-regulated proteins

The analysis of *M*-labelled proteins is described here in detail and the same analysis was applied to *H*-labelled proteins. The kinetic parameters were modelled as a linear model in logarithmic space using the following formula:

Control:

$$m_{syn\_con} = 10^{\alpha_0} \quad (5)$$

$$m_{deg\_con} = 10^{\beta_0} \quad (6)$$

Insulin:

$$m_{syn\_ins} = 10^{\alpha_0+\alpha_1} \quad (7)$$

$$m_{deg\_ins} = 10^{\beta_0+\beta_1} \quad (8)$$

Next, each protein was tested for whether it agreed with the hypothesis that there was a change in $[\dot{M}]$ when insulin was present (H_1), and therefore a change in m_{syn} or m_{deg}, or whether it agreed with the null hypothesis (H_0).

$$H_1: \alpha_1 \neq 0 \text{ or } \beta_1 \neq 0 \quad (9)$$

$$H_0: \alpha_1 = 0 \text{ or } \beta_1 = 0 \quad (10)$$

Proteins passed H_0 if the adjusted Coefficient of Determination ($adjR^2$) of the null hypothesis ($adjR_0^2$) is larger than that of the alternative hypothesis ($adjR_1^2$), because if $adjR_0^2 > adjR_1^2$, it implies the H_0 is a better fit to the data than H_1. This step also removes bias for H_1 generated by the increased degree of freedom in the model. For the remaining proteins, an F-statistic was obtained for the two models (H_1, H_0), using degrees of freedom $df_1 = 2$ and $df_2 = 15$. The F-statistic was converted to a p-value, which was adjusted for multiple comparisons testing using Benjamini-Hochberg algorithm in R (73,74). H_0 was rejected for proteins with a cut-off of $p <$

0.0005 for analysis of 'medium' and $p < 0.01$ for 'heavy' based on manual inspection for irregular time profiles of the resulting ranked list.

Statistical comparison of insulin and control m_{syn} and m_{deg} rates

Of the insulin-regulated proteins, which are those that rejected the null hypothesis above (9), we determined whether m_{syn}, m_{deg} or both parameters contributed to the changes with insulin. Expressed mathematically, we tested whether α_1, β_1 or both, were non-zero (5-8). We evaluated this hypothesis by examining the joint probability distributions of α_1 and β_1, this distribution illustrates the likely values of α_1 and β_1 (Fig. 6*C*). The joint probability distribution of α_1 and β_1 was generated by the following steps. Initially the joint likelihood distributions of α_0 and β_0 in the control conditions was constructed (Fig. 6*A*) from the following likelihood estimator equation:

$$L_{con}(\alpha_0, \beta_0) = \exp\{-\varepsilon_{con}(\alpha_0, \beta_0)/2\}$$

where ε_{con} is the sum of the squared residuals, weighted to the standard deviation. Similarly, the joint likelihood distribution of $\alpha_0+\alpha_1$ and $\beta_0+\beta_1$ under insulin conditions is given by

$$L_{ins}(\alpha_0 + \alpha_1, \beta_0 + \beta_1) = \exp\{-\varepsilon_{ins}(\alpha_0 + \alpha_1, \beta_0 + \beta_1)/2\}$$

Finally the joint likelihood distributions of α_0 and β_0 and of $\alpha_0+\alpha_1$ and $\beta_0+\beta_1$ were then used to construct the joint probability distribution for α_1 and β_1 as (Fig. 6*B*-*C*).

$$P(\alpha_1, \beta_1) = \frac{1}{E}\int_{-\infty}^{\infty}\int_{-\infty}^{\infty} L_{con}(\alpha_0, \beta_0) L_{ins}(\alpha_0 + \alpha_1, \beta_0 + \beta_1)\, d\alpha_0 d\beta_0 \quad (11)$$

where E, a normalisation factor, is defined as

$$E = \int_{-\infty}^{\infty}\int_{-\infty}^{\infty} P(\alpha_1, \beta_1)\, d\alpha_1 d\beta_1$$

Next, the marginal probability distribution for just the α_1 or β_1 variables were obtained by numerically integrating with respect to β_1 and α_1 respectively (Fig. 6*D*). The p-values for the marginal variables α_1 and β_1 were found by first calculating the distance between the mean and zero (Δ), then calculating the area under the curve outside the interval mean - Δ and mean + Δ (shaded area in Fig. 6*D*). The p-values were used to test the significance of the deviation of the marginal probabilities of α_1, β_1 from zero.

Gene ontology and Transcription factor analysis

Insulin-regulated proteins or long-lived proteins were analysed for enriched gene ontology categories ($p < 0.01$) using DAVID (75). Enriched transcription factors were identified through a hypergeometric test using the Molecular Signatures Database v4.0 (76)— "C3 motif gene set" (which is based on conserved cis-regulatory motifs between humans and other model organisms) curated from the TRANSFAC(77) database. Proteins that fit the models of synthesis with adj. $R^2 > 0.8$ were used as the background for this and p-value significance was defined by controlling for 5% FDR in this test.

Data quantification and general statistical analysis

Immunoblots were quantified by densitometry analysis using Image J software. T-tests and ANOVAs were done in GraphPad Prism version 6.01 for Windows (GraphPad Software).

Luciferase plasmids, transfection and luciferase assay

pCIneo-WT-Fluc and pCIneo-DM-Fluc were kindly provided by Dr Ulrich Hartl and Dr Swasti Raychaudhuri (Max Planck Institute) (49). pEGFP-N1 was from Clontech. pRK7-myc-Rheb was kindly provided by Dr John Blenis (Weill Cornell Medical College) (78). WT-Fluc and DM-Fluc were PCR-amplified and subcloned into pBabepuro. For stable overexpression, 3T3-L1 fibroblasts were infected with pBabepuro-WT-Fluc or pBabepuro-DM-Fluc retrovirus. HEK293 cells were co-transfected with pEGFP-N1 (Clontech) or pRK7-myc-Rheb in combination with pCIneo-WT-Fluc at 1:1 molar ratio using Lipofectamine 2000 (Thermo Scientific) according to the manufacturer's instructions for 6 h. After transfection, the culture media was replenished with DMEM FCS and cells treated with indicated drugs for 16 h and then harvested. To assay luciferase activity cells were lysed in 100 mM potassium phosphate pH 7.8 and 0.2 % Triton X-100 by passing through 27 G needle. Equivalent amounts of protein were assayed for luciferase activity with Luciferase Assay System (Promega).

Detergent insoluble proteins

Cells were lysed by passing through a 27 G needle in triton buffer (1% triton-X 100, 100 mM NaCl,

10 mM Tris, 10 uM MG132, 1 mM N-ethylmaleimide). Cell lysates were spun at 20,000 × g for 30 min at 4°C. The resulting pellet was transferred to a new Eppendorf tube, resuspended in triton buffer containing 30% sucrose by passing through a 27 G needle, and then spun for 100,000 × g for 30 min at 4°C. This step was repeated twice more to the cellular pellet. The final pellet was solubilised in 8 M urea, 2% SDS and 50 mM Tris by sonication and protein content determined by BCA assay.

Carbonylation

Protein carbonylation in freshly prepared extracts was measured by derivatisation of carbonyl groups with 2,4-dinitrophenylhydrazine (DNPH) followed by detection of DNP-derivatised protein by immunoblot using OxyBlot Protein Oxidation Detection Kit (S7150, Millipore). Membranes were then probed for tubulin and DNP-derivatised protein levels were normalised to tubulin levels.

Proteasome activity

Cells were solubilised by 5 min gentle agitation in proteasome lysis buffer (50 mM Tris pH 7.5, 250 mM sucrose, 5 mM $MgCl_2$, 2 mM ATP, 1mM DTT, 0.5 mM EDTA, 250 µg/ml digitonin). Samples with equivalent amounts of protein were assayed for proteasome activity with Proteasome-Glo™ Chymotrypsin-like Cell-Based Reagent (G8660, Promega).

Animals

Rat tissue was generated previously (46). Briefly, adult male Wistar rats were anesthetised and cannulas implanted into the right jugular vein and left carotid artery and exteriorised at the back of the neck. After surgery, rats were housed in separate cages and 3 d after surgery rats were infused with 0.9% saline or 50% glucose in water at 40 mg/kg/min via the carotid cannula using a peristaltic roller pump. After 1 d and 4 d of glucose infusion, rats were sacrificed and tissues rapidly dissected, frozen in liquid nitrogen and stored at -80°C. Animal experiments were approved by the Garvan Institute/ St Vincent's Hospital Animal Ethics Committee.

Data accessibility

All RAW and processed data associated with the manuscript has been deposited in PRIDE proteomeXchange (project accession PXD003696).

Acknowledgements: We thank members of the James laboratory, in particular Daniel Fazakerley, for valuable discussions, and Swasti Raychaudhuri for luciferase constructs. This study was supported by National Health and Medical Research Council (NHMRC) project grants GNT1061122 and GNT1086850 to D.E.J. The contents of the published material are solely the responsibility of the individual authors and do not reflect the view of NHMRC. D.E.J. is an NHMRC Senior Principal Research Fellow and A.Y.M is supported by an Australian Postgraduate Award scholarship.

Conflict of interest: The authors declare that they have no conflicts of interest with the contents of this article.

Author contributions: A.Y.M and D.E.J designed experiments and wrote the manuscript. A.Y.M performed the majority of the experiments. M.K.L.W. designed and performed the majority of the statistical analysis of proteomic data. R.C., J.Y.Y., A.C.F.C. contributed to the statistical analysis of protein turnover data. S.X.T. and J.S. assisted with study design. J.S. cloned DNA constructs. S.J.H. established MS methods. B.L.P. and S.J.H. ran MS samples. D.R.L and G.J.C. performed experiments on rats. All authors reviewed and edited the manuscript and approved the final version of the manuscript.

REFERENCES

1. Proud, C. G. (2006) Regulation of protein synthesis by insulin. *Biochemical Society transactions* **34**, 213-216
2. Ma, X. M., and Blenis, J. (2009) Molecular mechanisms of mTOR-mediated translational control. *Nature reviews. Molecular cell biology* **10**, 307-318
3. Shanik, M. H., Xu, Y., Skrha, J., Dankner, R., Zick, Y., and Roth, J. (2008) Insulin resistance and hyperinsulinemia: is hyperinsulinemia the cart or the horse? *Diabetes care* **31 Suppl 2**, S262-268
4. Mehran, A. E., Templeman, N. M., Brigidi, G. S., Lim, G. E., Chu, K. Y., Hu, X., Botezelli, J. D., Asadi, A., Hoffman, B. G., Kieffer, T. J., Bamji, S. X., Clee, S. M., and Johnson, J. D. (2012) Hyperinsulinemia drives diet-induced obesity independently of brain insulin production. *Cell metabolism* **16**, 723-737
5. Ortega-Molina, A., Lopez-Guadamillas, E., Mattison, J. A., Mitchell, S. J., Munoz-Martin, M., Iglesias, G., Gutierrez, V. M., Vaughan, K. L., Szarowicz, M. D., Gonzalez-Garcia, I., Lopez, M., Cebrian, D., Martinez, S., Pastor, J., de Cabo, R., and Serrano, M. (2015) Pharmacological inhibition of PI3K reduces adiposity and metabolic syndrome in obese mice and rhesus monkeys. *Cell metabolism* **21**, 558-570
6. Yang, X., Mei, S., Gu, H., Guo, H., Zha, L., Cai, J., Li, X., Liu, Z., and Cao, W. (2014) Exposure to excess insulin (glargine) induces type 2 diabetes mellitus in mice fed on a chow diet. *The Journal of endocrinology* **221**, 469-480
7. Selman, C., Lingard, S., Choudhury, A. I., Batterham, R. L., Claret, M., Clements, M., Ramadani, F., Okkenhaug, K., Schuster, E., Blanc, E., Piper, M. D., Al-Qassab, H., Speakman, J. R., Carmignac, D., Robinson, I. C., Thornton, J. M., Gems, D., Partridge, L., and Withers, D. J. (2008) Evidence for lifespan extension and delayed age-related biomarkers in insulin receptor substrate 1 null mice. *FASEB journal : official publication of the Federation of American Societies for Experimental Biology* **22**, 807-818
8. Holzenberger, M., Dupont, J., Ducos, B., Leneuve, P., Geloen, A., Even, P. C., Cervera, P., and Le Bouc, Y. (2003) IGF-1 receptor regulates lifespan and resistance to oxidative stress in mice. *Nature* **421**, 182-187
9. Tatar, M., Kopelman, A., Epstein, D., Tu, M. P., Yin, C. M., and Garofalo, R. S. (2001) A mutant Drosophila insulin receptor homolog that extends life-span and impairs neuroendocrine function. *Science* **292**, 107-110
10. Finkel, T. (2015) The metabolic regulation of aging. *Nature medicine* **21**, 1416-1423
11. Hands, S. L., Proud, C. G., and Wyttenbach, A. (2009) mTOR's role in ageing: protein synthesis or autophagy? *Aging* **1**, 586-597
12. Cohen, E., and Dillin, A. (2008) The insulin paradox: aging, proteotoxicity and neurodegeneration. *Nature reviews. Neuroscience* **9**, 759-767
13. Ozcan, U., Cao, Q., Yilmaz, E., Lee, A. H., Iwakoshi, N. N., Ozdelen, E., Tuncman, G., Gorgun, C., Glimcher, L. H., and Hotamisligil, G. S. (2004) Endoplasmic reticulum stress links obesity, insulin action, and type 2 diabetes. *Science* **306**, 457-461
14. Otoda, T., Takamura, T., Misu, H., Ota, T., Murata, S., Hayashi, H., Takayama, H., Kikuchi, A., Kanamori, T., Shima, K. R., Lan, F., Takeda, T., Kurita, S., Ishikura, K., Kita, Y., Iwayama, K., Kato, K., Uno, M., Takeshita, Y., Yamamoto, M., Tokuyama, K., Iseki, S., Tanaka, K., and Kaneko, S. (2013) Proteasome dysfunction mediates obesity-induced endoplasmic reticulum stress and insulin resistance in the liver. *Diabetes* **62**, 811-824
15. Yang, L., Li, P., Fu, S., Calay, E. S., and Hotamisligil, G. S. (2010) Defective hepatic autophagy in obesity promotes ER stress and causes insulin resistance. *Cell metabolism* **11**, 467-478
16. Bjedov, I., Toivonen, J. M., Kerr, F., Slack, C., Jacobson, J., Foley, A., and Partridge, L. (2010) Mechanisms of life span extension by rapamycin in the fruit fly Drosophila melanogaster. *Cell metabolism* **11**, 35-46

17. Hipp, M. S., Park, S. H., and Hartl, F. U. (2014) Proteostasis impairment in protein-misfolding and -aggregation diseases. *Trends in cell biology* **24**, 506-514
18. Kaushik, S., and Cuervo, A. M. (2015) Proteostasis and aging. *Nature medicine* **21**, 1406-1415
19. Demontis, F., and Perrimon, N. (2010) FOXO/4E-BP signaling in Drosophila muscles regulates organism-wide proteostasis during aging. *Cell* **143**, 813-825
20. Taylor, R. C., Berendzen, K. M., and Dillin, A. (2014) Systemic stress signalling: understanding the cell non-autonomous control of proteostasis. *Nature reviews. Molecular cell biology* **15**, 211-217
21. Tan, S. X., Fisher-Wellman, K. H., Fazakerley, D. J., Ng, Y., Pant, H., Li, J., Meoli, C. C., Coster, A. C., Stockli, J., and James, D. E. (2015) Selective insulin resistance in adipocytes. *The Journal of biological chemistry* **290**, 11337-11348
22. Walther, D. M., Kasturi, P., Zheng, M., Pinkert, S., Vecchi, G., Ciryam, P., Morimoto, R. I., Dobson, C. M., Vendruscolo, M., Mann, M., and Hartl, F. U. (2015) Widespread Proteome Remodeling and Aggregation in Aging C. elegans. *Cell* **161**, 919-932
23. Ong, S. E., Blagoev, B., Kratchmarova, I., Kristensen, D. B., Steen, H., Pandey, A., and Mann, M. (2002) Stable isotope labeling by amino acids in cell culture, SILAC, as a simple and accurate approach to expression proteomics. *Molecular & cellular proteomics : MCP* **1**, 376-386
24. Schwanhausser, B., Gossen, M., Dittmar, G., and Selbach, M. (2009) Global analysis of cellular protein translation by pulsed SILAC. *Proteomics* **9**, 205-209
25. Selbach, M., Schwanhausser, B., Thierfelder, N., Fang, Z., Khanin, R., and Rajewsky, N. (2008) Widespread changes in protein synthesis induced by microRNAs. *Nature* **455**, 58-63
26. Iadevaia, V., Huo, Y., Zhang, Z., Foster, L. J., and Proud, C. G. (2012) Roles of the mammalian target of rapamycin, mTOR, in controlling ribosome biogenesis and protein synthesis. *Biochemical Society transactions* **40**, 168-172
27. Kristensen, A. R., Gsponer, J., and Foster, L. J. (2013) Protein synthesis rate is the predominant regulator of protein expression during differentiation. *Molecular systems biology* **9**, 689
28. Gawron, D., Ndah, E., Gevaert, K., and Van Damme, P. (2016) Positional proteomics reveals differences in N-terminal proteoform stability. *Molecular systems biology* **12**, 858
29. Hoehn, K. L., Hohnen-Behrens, C., Cederberg, A., Wu, L. E., Turner, N., Yuasa, T., Ebina, Y., and James, D. E. (2008) IRS1-independent defects define major nodes of insulin resistance. *Cell metabolism* **7**, 421-433
30. Abel, E. D., Peroni, O., Kim, J. K., Kim, Y. B., Boss, O., Hadro, E., Minnemann, T., Shulman, G. I., and Kahn, B. B. (2001) Adipose-selective targeting of the GLUT4 gene impairs insulin action in muscle and liver. *Nature* **409**, 729-733
31. Ruan, H., Zarnowski, M. J., Cushman, S. W., and Lodish, H. F. (2003) Standard isolation of primary adipose cells from mouse epididymal fat pads induces inflammatory mediators and down-regulates adipocyte genes. *The Journal of biological chemistry* **278**, 47585-47593
32. Govers, R., Coster, A. C., and James, D. E. (2004) Insulin increases cell surface GLUT4 levels by dose dependently discharging GLUT4 into a cell surface recycling pathway. *Molecular and cellular biology* **24**, 6456-6466
33. Boisvert, F. M., Ahmad, Y., Gierlinski, M., Charriere, F., Lamont, D., Scott, M., Barton, G., and Lamond, A. I. (2012) A quantitative spatial proteomics analysis of proteome turnover in human cells. *Molecular & cellular proteomics : MCP* **11**, M111 011429
34. Robles, M. S., Cox, J., and Mann, M. (2014) In-vivo quantitative proteomics reveals a key contribution of post-transcriptional mechanisms to the circadian regulation of liver metabolism. *PLoS genetics* **10**, e1004047
35. Alexander, M., Curtis, G., Avruch, J., and Goodman, H. M. (1985) Insulin regulation of protein biosynthesis in differentiated 3T3 adipocytes. Regulation of glyceraldehyde-3-phosphate dehydrogenase. *The Journal of biological chemistry* **260**, 11978-11985

36. Ong, J. M., Kirchgessner, T. G., Schotz, M. C., and Kern, P. A. (1988) Insulin increases the synthetic rate and messenger RNA level of lipoprotein lipase in isolated rat adipocytes. *The Journal of biological chemistry* **263**, 12933-12938
37. Sargeant, R. J., and Paquet, M. R. (1993) Effect of insulin on the rates of synthesis and degradation of GLUT1 and GLUT4 glucose transporters in 3T3-L1 adipocytes. *The Biochemical journal* **290 (Pt 3)**, 913-919
38. Conn, C. S., and Qian, S. B. (2013) Nutrient signaling in protein homeostasis: an increase in quantity at the expense of quality. *Science signaling* **6**, ra24
39. Ozcan, U., Ozcan, L., Yilmaz, E., Duvel, K., Sahin, M., Manning, B. D., and Hotamisligil, G. S. (2008) Loss of the tuberous sclerosis complex tumor suppressors triggers the unfolded protein response to regulate insulin signaling and apoptosis. *Molecular cell* **29**, 541-551
40. Tyagi, R., Shahani, N., Gorgen, L., Ferretti, M., Pryor, W., Chen, P. Y., Swarnkar, S., Worley, P. F., Karbstein, K., Snyder, S. H., and Subramaniam, S. (2015) Rheb Inhibits Protein Synthesis by Activating the PERK-eIF2alpha Signaling Cascade. *Cell reports*
41. Hein, M. Y., Hubner, N. C., Poser, I., Cox, J., Nagaraj, N., Toyoda, Y., Gak, I. A., Weisswange, I., Mansfeld, J., Buchholz, F., Hyman, A. A., and Mann, M. (2015) A human interactome in three quantitative dimensions organized by stoichiometries and abundances. *Cell* **163**, 712-723
42. Okabayashi, Y., Maddux, B. A., McDonald, A. R., Logsdon, C. D., Williams, J. A., and Goldfine, I. D. (1989) Mechanisms of insulin-induced insulin-receptor downregulation. Decrease of receptor biosynthesis and mRNA levels. *Diabetes* **38**, 182-187
43. Toyama, B. H., Savas, J. N., Park, S. K., Harris, M. S., Ingolia, N. T., Yates, J. R., 3rd, and Hetzer, M. W. (2013) Identification of long-lived proteins reveals exceptional stability of essential cellular structures. *Cell* **154**, 971-982
44. Teixeira, L. K., and Reed, S. I. (2013) Ubiquitin ligases and cell cycle control. *Annual review of biochemistry* **82**, 387-414
45. Lin, J. H., Li, H., Yasumura, D., Cohen, H. R., Zhang, C., Panning, B., Shokat, K. M., Lavail, M. M., and Walter, P. (2007) IRE1 signaling affects cell fate during the unfolded protein response. *Science* **318**, 944-949
46. Laybutt, D. R., Chisholm, D. J., and Kraegen, E. W. (1997) Specific adaptations in muscle and adipose tissue in response to chronic systemic glucose oversupply in rats. *The American journal of physiology* **273**, E1-9
47. Humphrey, S. J., Yang, G., Yang, P., Fazakerley, D. J., Stockli, J., Yang, J. Y., and James, D. E. (2013) Dynamic adipocyte phosphoproteome reveals that Akt directly regulates mTORC2. *Cell metabolism* **17**, 1009-1020
48. Frydman, J., Erdjument-Bromage, H., Tempst, P., and Hartl, F. U. (1999) Co-translational domain folding as the structural basis for the rapid de novo folding of firefly luciferase. *Nature structural biology* **6**, 697-705
49. Gupta, R., Kasturi, P., Bracher, A., Loew, C., Zheng, M., Villella, A., Garza, D., Hartl, F. U., and Raychaudhuri, S. (2011) Firefly luciferase mutants as sensors of proteome stress. *Nature methods* **8**, 879-884
50. Cohen, E., Paulsson, J. F., Blinder, P., Burstyn-Cohen, T., Du, D., Estepa, G., Adame, A., Pham, H. M., Holzenberger, M., Kelly, J. W., Masliah, E., and Dillin, A. (2009) Reduced IGF-1 signaling delays age-associated proteotoxicity in mice. *Cell* **139**, 1157-1169
51. King, M. A., Hands, S., Hafiz, F., Mizushima, N., Tolkovsky, A. M., and Wyttenbach, A. (2008) Rapamycin inhibits polyglutamine aggregation independently of autophagy by reducing protein synthesis. *Molecular pharmacology* **73**, 1052-1063
52. Cohen, E., Bieschke, J., Perciavalle, R. M., Kelly, J. W., and Dillin, A. (2006) Opposing activities protect against age-onset proteotoxicity. *Science* **313**, 1604-1610
53. David, D. C., Ollikainen, N., Trinidad, J. C., Cary, M. P., Burlingame, A. L., and Kenyon, C. (2010) Widespread protein aggregation as an inherent part of aging in C. elegans. *PLoS biology* **8**, e1000450

54. Novosyadlyy, R., Kurshan, N., Lann, D., Vijayakumar, A., Yakar, S., and LeRoith, D. (2008) Insulin-like growth factor-I protects cells from ER stress-induced apoptosis via enhancement of the adaptive capacity of endoplasmic reticulum. *Cell death and differentiation* **15**, 1304-1317
55. Humbert, S., Bryson, E. A., Cordelieres, F. P., Connors, N. C., Datta, S. R., Finkbeiner, S., Greenberg, M. E., and Saudou, F. (2002) The IGF-1/Akt pathway is neuroprotective in Huntington's disease and involves Huntingtin phosphorylation by Akt. *Developmental cell* **2**, 831-837
56. Di Carlo, M., Picone, P., Carrotta, R., Giacomazza, D., and San Biagio, P. L. (2010) Insulin promotes survival of amyloid-beta oligomers neuroblastoma damaged cells via caspase 9 inhibition and Hsp70 upregulation. *Journal of biomedicine & biotechnology* **2010**, 147835
57. Carro, E., Trejo, J. L., Gomez-Isla, T., LeRoith, D., and Torres-Aleman, I. (2002) Serum insulin-like growth factor I regulates brain amyloid-beta levels. *Nature medicine* **8**, 1390-1397
58. Zhang, Y., Nicholatos, J., Dreier, J. R., Ricoult, S. J., Widenmaier, S. B., Hotamisligil, G. S., Kwiatkowski, D. J., and Manning, B. D. (2014) Coordinated regulation of protein synthesis and degradation by mTORC1. *Nature* **513**, 440-443
59. Riley, B. E., Kaiser, S. E., Shaler, T. A., Ng, A. C., Hara, T., Hipp, M. S., Lage, K., Xavier, R. J., Ryu, K. Y., Taguchi, K., Yamamoto, M., Tanaka, K., Mizushima, N., Komatsu, M., and Kopito, R. R. (2010) Ubiquitin accumulation in autophagy-deficient mice is dependent on the Nrf2-mediated stress response pathway: a potential role for protein aggregation in autophagic substrate selection. *The Journal of cell biology* **191**, 537-552
60. Simonsen, A., Cumming, R. C., Brech, A., Isakson, P., Schubert, D. R., and Finley, K. D. (2008) Promoting basal levels of autophagy in the nervous system enhances longevity and oxidant resistance in adult Drosophila. *Autophagy* **4**, 176-184
61. Chou, S. D., Prince, T., Gong, J., and Calderwood, S. K. (2012) mTOR is essential for the proteotoxic stress response, HSF1 activation and heat shock protein synthesis. *PloS one* **7**, e39679
62. Santagata, S., Mendillo, M. L., Tang, Y. C., Subramanian, A., Perley, C. C., Roche, S. P., Wong, B., Narayan, R., Kwon, H., Koeva, M., Amon, A., Golub, T. R., Porco, J. A., Jr., Whitesell, L., and Lindquist, S. (2013) Tight coordination of protein translation and HSF1 activation supports the anabolic malignant state. *Science* **341**, 1238303
63. Boden, G., and Merali, S. (2011) Measurement of the increase in endoplasmic reticulum stress-related proteins and genes in adipose tissue of obese, insulin-resistant individuals. *Methods in enzymology* **489**, 67-82
64. Boden, G., Cheung, P., Salehi, S., Homko, C., Loveland-Jones, C., Jayarajan, S., Stein, T. P., Williams, K. J., Liu, M. L., Barrero, C. A., and Merali, S. (2014) Insulin regulates the unfolded protein response in human adipose tissue. *Diabetes* **63**, 912-922
65. Gregor, M. F., and Hotamisligil, G. S. (2007) Thematic review series: Adipocyte Biology. Adipocyte stress: the endoplasmic reticulum and metabolic disease. *Journal of lipid research* **48**, 1905-1914
66. Urano, F., Wang, X., Bertolotti, A., Zhang, Y., Chung, P., Harding, H. P., and Ron, D. (2000) Coupling of stress in the ER to activation of JNK protein kinases by transmembrane protein kinase IRE1. *Science* **287**, 664-666
67. Winnay, J. N., Boucher, J., Mori, M. A., Ueki, K., and Kahn, C. R. (2010) A regulatory subunit of phosphoinositide 3-kinase increases the nuclear accumulation of X-box-binding protein-1 to modulate the unfolded protein response. *Nature medicine* **16**, 438-445
68. Park, S. W., Zhou, Y., Lee, J., Lu, A., Sun, C., Chung, J., Ueki, K., and Ozcan, U. (2010) The regulatory subunits of PI3K, p85alpha and p85beta, interact with XBP-1 and increase its nuclear translocation. *Nature medicine* **16**, 429-437
69. Schwanhausser, B., Busse, D., Li, N., Dittmar, G., Schuchhardt, J., Wolf, J., Chen, W., and Selbach, M. (2011) Global quantification of mammalian gene expression control. *Nature* **473**, 337-342

70. Wisniewski, J. R., Zougman, A., and Mann, M. (2009) Combination of FASP and StageTip-based fractionation allows in-depth analysis of the hippocampal membrane proteome. *Journal of proteome research* **8**, 5674-5678
71. Cox, J., and Mann, M. (2008) MaxQuant enables high peptide identification rates, individualized p.p.b.-range mass accuracies and proteome-wide protein quantification. *Nature biotechnology* **26**, 1367-1372
72. Cox, J., Neuhauser, N., Michalski, A., Scheltema, R. A., Olsen, J. V., and Mann, M. (2011) Andromeda: a peptide search engine integrated into the MaxQuant environment. *Journal of proteome research* **10**, 1794-1805
73. Benjamini, Y., Drai, D., Elmer, G., Kafkafi, N., and Golani, I. (2001) Controlling the false discovery rate in behavior genetics research. *Behavioural brain research* **125**, 279-284
74. R Development Core Team. (2008) R: A Language and Environment for Statistical Computing. R Foundation for Statistical Computing, Vienna, Austria
75. Huang da, W., Sherman, B. T., and Lempicki, R. A. (2009) Systematic and integrative analysis of large gene lists using DAVID bioinformatics resources. *Nature protocols* **4**, 44-57
76. Subramanian, A., Tamayo, P., Mootha, V. K., Mukherjee, S., Ebert, B. L., Gillette, M. A., Paulovich, A., Pomeroy, S. L., Golub, T. R., Lander, E. S., and Mesirov, J. P. (2005) Gene set enrichment analysis: a knowledge-based approach for interpreting genome-wide expression profiles. *Proceedings of the National Academy of Sciences of the United States of America* **102**, 15545-15550
77. Matys, V., Kel-Margoulis, O. V., Fricke, E., Liebich, I., Land, S., Barre-Dirrie, A., Reuter, I., Chekmenev, D., Krull, M., Hornischer, K., Voss, N., Stegmaier, P., Lewicki-Potapov, B., Saxel, H., Kel, A. E., and Wingender, E. (2006) TRANSFAC and its module TRANSCompel: transcriptional gene regulation in eukaryotes. *Nucleic acids research* **34**, D108-110
78. Tee, A. R., Manning, B. D., Roux, P. P., Cantley, L. C., and Blenis, J. (2003) Tuberous sclerosis complex gene products, Tuberin and Hamartin, control mTOR signaling by acting as a GTPase-activating protein complex toward Rheb. *Current biology : CB* **13**, 1259-1268

FOOTNOTES

[1]The Garvan Institute of Medical Research, Sydney, NSW 2010, Australia
[2]Charles Perkins Centre, School of Life Environmental Sciences, University of Sydney, Sydney, NSW 2006, Australia
[3]School of Physics, University of Sydney, Sydney, NSW 2006, Australia
[4]School of Mathematics and Statistics, University of Sydney, Sydney, NSW, 2006, Australia
[5]Department of Applied Mathematics, School of Mathematics and Statistics, University of New South Wales, Sydney, NSW 2052, Australia
[6]School of Medicine, University of Sydney, Sydney, NSW 2006, Australia
*Present address: Republic Polytechnic, Singapore.
[7]To whom correspondence should be addressed: David E. James, Charles Perkins Centre, School of Life Environmental Sciences, University of Sydney, Sydney, NSW 2006, Australia, Tel.: +61 2 8627 1621, E-mail: david.james@sydney.edu.au
[8]Abbreviations used: ISP, insulin signalling pathway; ER, endoplasmic reticulum; SILAC, stable isotope labelled amino acids in cell culture; M, medium isotopes; L, light isotopes; H, light isotopes; m_{syn}, synthesis rate of M; m_{deg}, degradation rate of M; h_{syn}, synthesis rate of H; h_{deg}, degradation rate of H.

FIGURE LEGENDS

FIGURE 1. Analysis of insulin-stimulated protein synthesis and degradation by pulse-chase SILAC and mass spectrometry. (A) Schematic of pulse-chase SILAC experiment. 3T3-L1 adipocytes were labelled with 'heavy' (H) and pulsed with 'medium' (M) isotopes of arginine and lysine. After switching to medium, cells were harvested after 6, 12, 24, 48 h in the first experiment, and after 6, 12, 24, 48, 72, 96 h in the second experiment. Adipocytes were then mixed with 'light' (L) labelled adipocytes and the amount of H, M, L labelled proteins analysed by shot-gun proteomics. **(B)** Protein/DNA ratio was quantified in 3T3-L1 adipocytes treated with insulin for indicated days and normalised to untreated cells (indicated by dotted line) (n = 4, mean ± S.E.M., one-sample t-test, * $p < 0.05$). **(C)** 3T3-L1 adipocytes were treated with insulin for indicated days and lysates immunoblotted with phospho-S6 (S235/S236) and 14-3-3 (loading control) antibodies. Immunoblots were quantified and normalised to the loading control and untreated cells (indicated by dotted line) (n = 6, mean ± S.E.M., one-sample t-test, * $p < 0.05$). **(D)** Boxplots of histone protein abundance quantified in pulse-chase SILAC experiment relative to time = 0 for control and insulin-treated cells (n = 9 proteins) of 2 independent experiments. **(E)** Global change in M and H proteins in control and insulin-treated samples during pulse-chase SILAC experiment. Shading indicates interquartile range and line indicates median.

FIGURE 2. Insulin up-regulates synthesis and stability of newly made proteins. (A) Number of proteins that were quantified, curve-fitted or insulin-regulated in protein synthesis data. **(B)** Graph of abundance of representative 'medium'-labelled proteins over the time course in control and insulin-treated cells. Line indicates best fit synthesis curve. Bar graph indicates mean and S.D. of the curve parameters m_{syn} for synthesis and m_{deg} for degradation of newly synthesised protein (* $p < 0.05$). **(C)** Relative abundance of significantly insulin-regulated proteins relative to control samples 48 h post chase. **(D)** Bar chart of insulin-regulated proteins with significantly increased or decreased ($p < 0.05$) m_{syn} or m_{deg}. **(B & D)** Statistics were performed on linearised model as described in *experimental procedures*.

FIGURE 3. Insulin minimally affects protein degradation despite suppression of autophagy. (A) Number of proteins that were quantified, curve-fitted, insulin-regulated or long-lived in protein degradation data. **(B)** Gene ontology (GO) terms of long-lived proteins from proteomic data with number of proteins in each category in brackets. Significantly enriched GO terms are indicated (* $p < 0.05$). **(C)** Graph of abundance of representative 'heavy'-labelled proteins in control and insulin-treated cells over the time course. Line indicates best-fit degradation curve. Bar graph indicates mean and S.D. of the curve parameters h_{deg} for degradation and h_{syn} for reincorporation of 'heavy' amino acids into proteins. Statistics were performed on linearised model as described in *experimental procedures* (* $p < 0.05$). **(D)** Density graph of proteome half-lives calculated from protein degradation data. **(E)** 3T3-L1 adipocytes were treated with insulin for indicated times or MG132 for 2 h. Chymotrypsin activity of 26S proteasome was quantified and normalised to untreated cells (indicated by dotted line) (n = 4, mean ± S.E.M., one-sample t-test, * $p < 0.05$). **(F)** 3T3-L1 adipocytes were treated with insulin for indicated days and/or 400 μM chloroquine for 15 min. Cell lysates were immunoblotted with indicated antibodies. Vertical lines on immunoblots indicate where blot was spliced. Immunoblots were quantified and LC3-II normalised to the 14-3-3 loading control. LC3-II flux was calculated as the difference of LC3-II with chloroquine minus without chloroquine for each time point (n = 5, mean ± S.E.M., one-sample t-test, * $p < 0.05$).

FIGURE 4. Insulin coordinates synthesis of proteins across multiple compartments with proteostasis network. (A) Gene ontology of newly-made proteins significantly increased in response to insulin are highlighted in red and depicted in the illustration of a cell. Bar graphs depict the percentage increase in abundance of ER UPR, mitochondrial (mito) UPR or cytosolic chaperone proteins synthesised after 48 h incubation with insulin compared to control. Black bars indicate significantly insulin-regulated proteins. Blue horizontal bar indicates the interquartile-range of the percentage increase in insulin-regulated proteins. **(B)** 3T3-L1 adipocytes were treated with insulin for 24 h and cell lysates immunoblotted for indicated proteins. Immunoblots were quantified and normalised to loading control and untreated samples (n = 5 for pIRE1 and pEIF2α, n = 3 for pPERK, mean ± S.E.M., one-sample t-test, * $p < 0.05$). **(C-D)** Rats were cannulated and infused with 40 mg/kg/min glucose for indicated periods or

saline for 4 d. **(C)** Plasma glucose and insulin levels are reproduced from Laybutt et al. 1997. **(D)** Adipose tissue of rats were immunoblotted for indicated protein. Immunoblots were quantified and normalised to loading control and saline samples (n = 4, mean ± S.E.M., two-sample t-test, * $p < 0.05$). **(E)** 3T3-L1 adipocytes were serum starved for 1.5 h and treated with insulin for indicated times. Cell lysates were immunoblotted with indicated antibodies. Immunoblots were quantified and normalised to 14-3-3. Data was scaled so that basal is set to 0 and maximal response set to 1 (n = 4, mean ± S.E.M., one-sample t-test, * $p < 0.05$). **(F & G)** 3T3-L1 adipocytes were serum starved for 1.5 h, treated with indicted inhibitors for 30 min, followed by insulin for 30 min. Cell lysates were immunoblotted for indicated proteins. Vertical lines on immunoblots indicate where blot was spliced. Immunoblots were quantified and normalised to 14-3-3. Insulin-stimulated pIRE1 is expressed as fold change relative to DMSO treated samples (indicated by dotted line) (F n = 4, G n = 5, mean ± S.E.M., one-sample t-test, * $p < 0.05$).

FIGURE 5. Insulin preserves protein folding. (A) 3T3-L1 adipocytes were treated with insulin for indicated periods or MG132 for 24 h. Triton X-100 insoluble protein was measured and normalised to untreated cells (indicated by dotted line) (n = 3, mean ± S.E.M., one-sample t-test, * $p < 0.05$). **(B)** Triton X-100 insoluble protein relative to total protein was measured in adipose tissue of rats (Fig. 4*C*) (saline n = 6, 1 d glucose n = 8, 4 d glucose n = 7, mean ± S.E.M., two-sample t-test, * $p < 0.05$). **(C)** 3T3-L1 adipocytes were treated with insulin for indicated periods or H_2O_2 for 30 min. Carbonylation was measured and normalised to untreated cells (n = 3, mean ± S.E.M., one-sample t-test, * $p < 0.05$). **(D)** Carbonylation was measured in rats (Fig. 4C) (saline n = 6, 1 d glucose n = 8, 4 d glucose n = 7, mean ± S.E.M., two-sample t-test, * $p < 0.05$). **(E)** 3T3-L1 adipocytes stably expressing WT Fluc or DM Fluc were assayed for luminescence. Luminescence was normalised to cells expressing WT Fluc (n = 4, mean ± S.E.M., one-sample t-test, * $p < 0.05$). **(F, G)** 3T3-L1 adipocytes stably expressing WT Fluc **(F)** or DM Fluc **(G)** were treated with insulin for indicated periods and assayed for luminescence. Luminescence was normalised to untreated cells (indicated by dotted line). (F n = 4, G n = 6, mean ± S.E.M., one-sample t-test, * $p < 0.05$). **(H)** 3T3-L1 adipocytes stably expressing DM Fluc were treated with insulin and/or rapamycin for 24 h and assayed for luminescence. Luminescence was normalised to untreated cells (indicated by dotted line) (n = 3, mean ± S.E.M., one-way ANOVA, * $p < 0.05$). **(I-K)** HEK293 cells were transiently co-transfected with WT Fluc and either EGFP or Rheb-Myc, and treated with insulin and/or rapamycin for 24 h. Lysates were immunoblotted with indicated antibodies **(I)**, quantified and normalised to 14-3-3 and untreated sample expressing EGFP (indicated by dotted line) **(J)** (n = 3, mean ± S.E.M., one-sample t-test, * $p < 0.05$). Luminescence was measured in separate cells and normalised to untreated sample expressing EGFP **(K)** (n = 4, mean ± S.E.M., one-sample t-test, * $p < 0.05$).

FIGURE 6. Sensitivity analysis of synthesis and degradation parameters to determine significance of their change using maximum likelihood. (A) The joint likelihood distribution of **(i)** control with respect to α_0 and β_0, corresponding to m_{syn_con} and m_{deg_con}, respectively, and **(ii)** insulin with respect to $\alpha_0 + \alpha_1$ and $\beta_0 + \beta_1$, corresponding to m_{syn_ins} and m_{deg_ins}, respectively. **(B)** The joint likelihoods for control and insulin are superimposed, their likelihoods multiplied and then summed across the entire landscape to form one grid point in the joint likelihood distribution for α_1 and β_1 (Eqn 11). Each subsequent grid point in the joint likelihood distribution for α_1 and β_1 is determined by repeating the process but shifting the joint likelihood for insulin in the x and y directions. **(C)** After performing the operation described in (B) for all possible offsets between the control and insulin joint likelihoods, the joint likelihood for the parameter change is formed. **(D)** The marginalised probability distribution for α_1 and β_1, the change in the synthesis and degradation rate, respectively, are obtained by first marginalising the joint likelihood distribution in (C), then normalising the integral to 1. The p-value is represented by the blue area under the curve and is a measure of the distance of the distribution away from zero.

FIGURES

FIGURE 1.

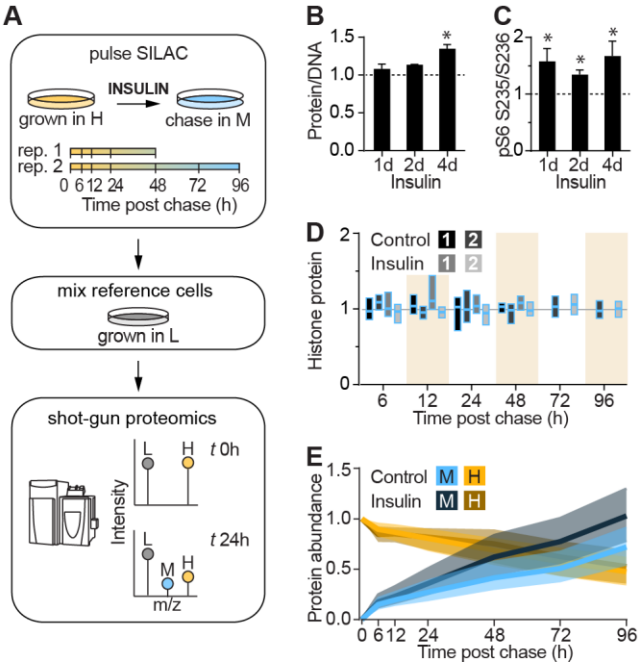

FIGURE 2.

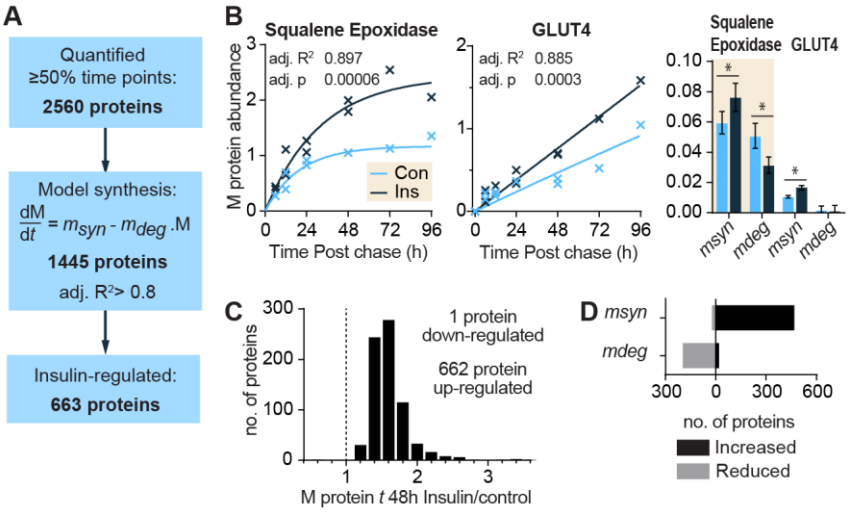

FIGURE 3.

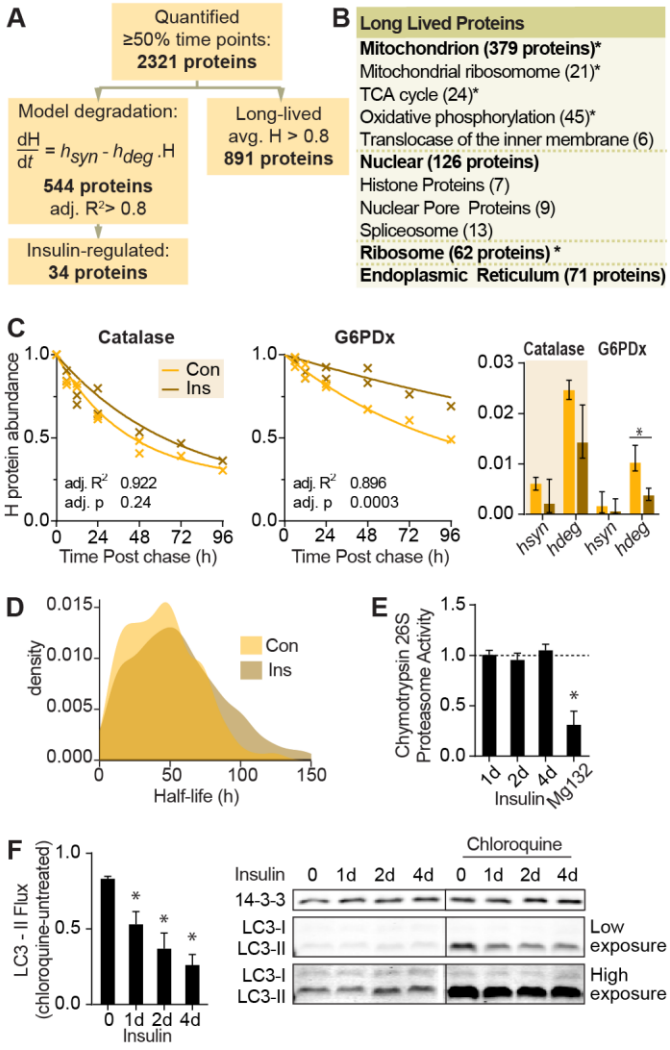

FIGURE 4.

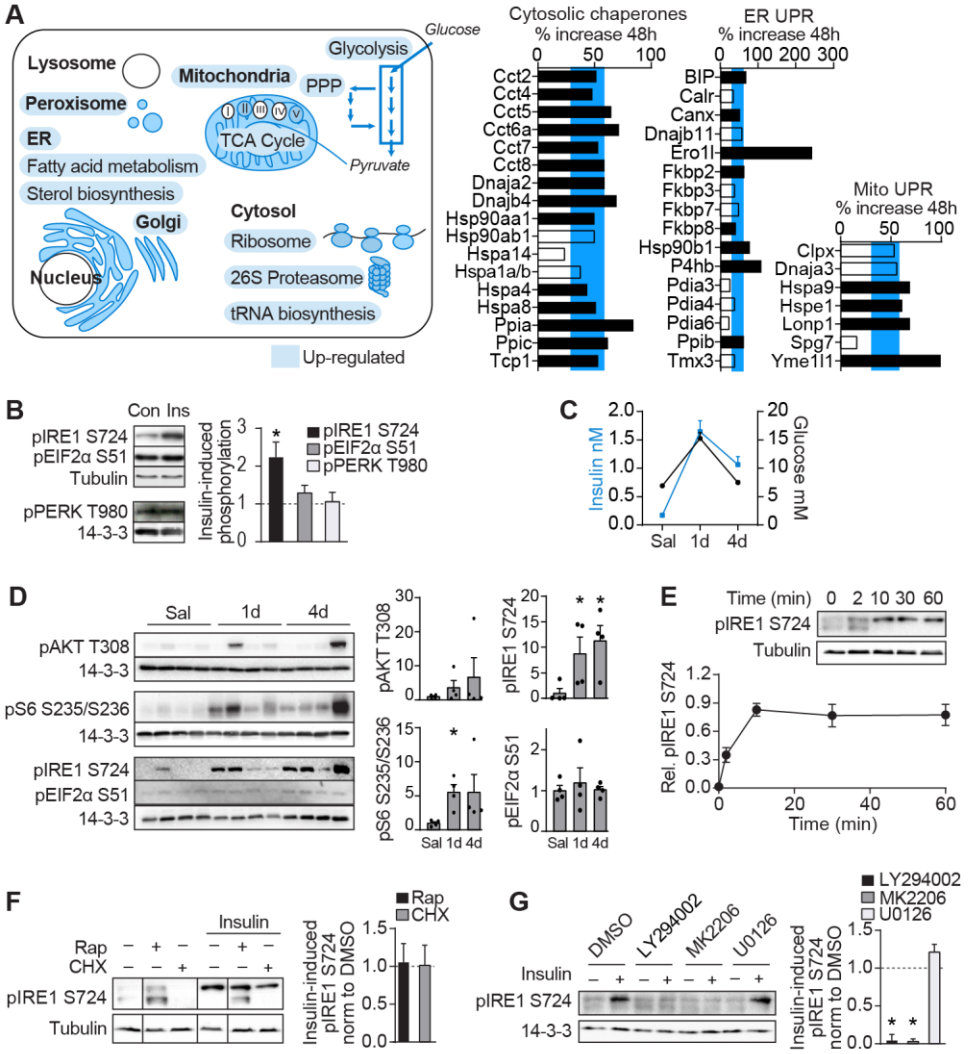

FIGURE 5

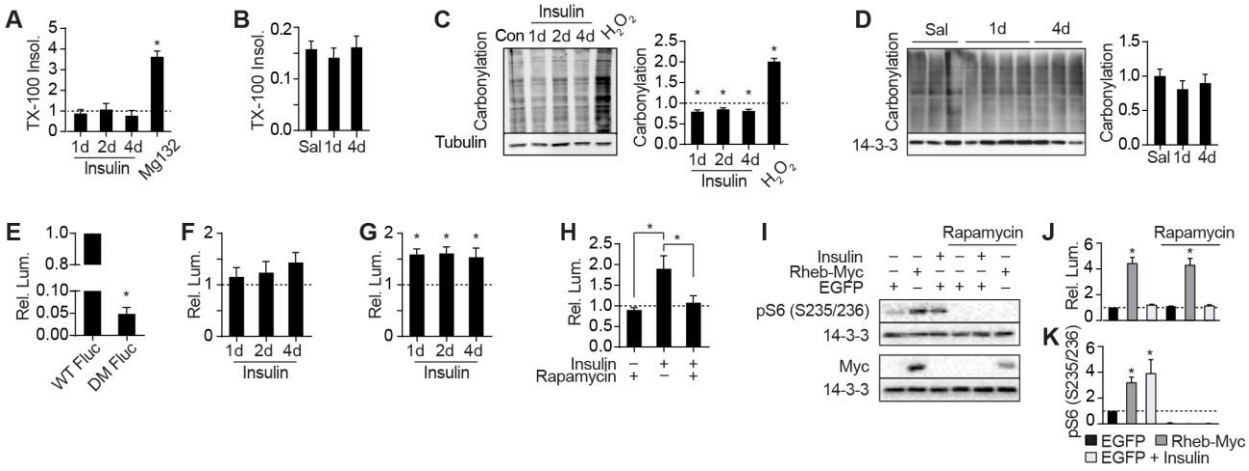

FIGURE 6

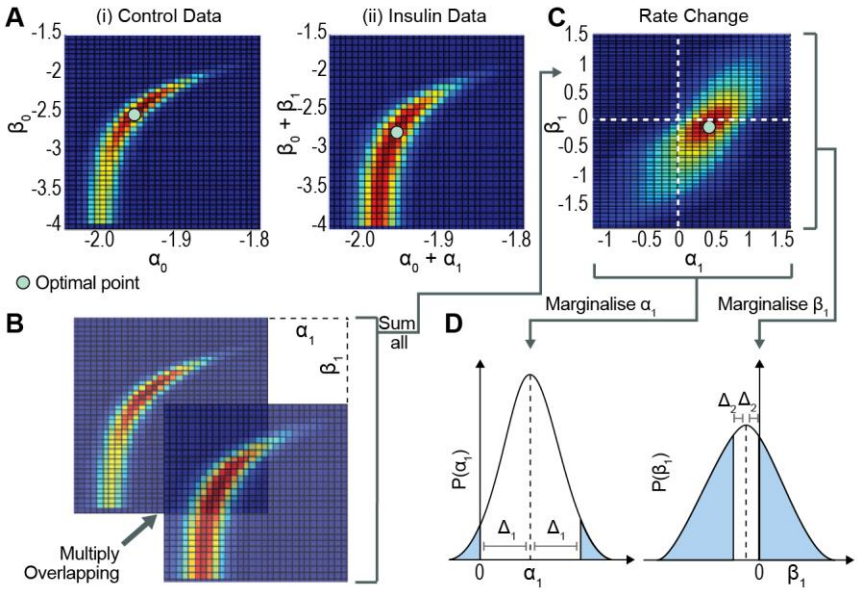

Hyper-activation of the Insulin Signaling Pathway Improves Intracellular Proteostasis by Coordinately Upregulating the Proteostatic Machinery in Adipocytes

Annabel Y. Minard, Martin K. L. Wong, Rima Chaudhuri, Shi-Xiong Tan, Sean J. Humphrey, Benjamin L. Parker, Jean Y. Yang, D. Ross Laybutt, Gregory J. Cooney, Adelle C. F. Coster, Jacqueline Stoeckli and David E. James

J. Biol. Chem. published online October 13, 2016
